CONTROL OF THE SPATIAL STRUCTURE OF A LASER-PRODUCED PLASMA CLOUD AS IT EXPANDS INTO A VACUUM

A. M. Orishich, A. G. Ponomarenko, and V. N. Snytnikov

UDC 533.601+533.95

The spherical cloud of a laser-produced plasma is most suitable for studying a number of fundamental processes in plasma physics, including the interaction of a moving plasma with a magnetic field and with a magnetized medium, collective acceleration of ions, and the "anomalous" ionization of a neutral gas [1]. To use the plasma cloud it is necessary to know the laws governing the expansion of the plasma into a vacuum; the study of these laws is also of interest in itself, owing to the work on laser-driven fusion [2], laboratory modeling of explosive astrophysical phenomena, and other applications [3].

The numerous studies of laser-produced plasma follow three basic directions. The first direction, associated with laser-driven fusion, involves the study of the dynamics of matter near the target with a plasma concentration of the order of the critical value $n_* = \rho_*/M = m\omega^2/4\pi e^2$ for radiation with frequency ω (M is the mass of the background ions). Different aspects of plasma flow in this case can be described by quasistationary hydrodynamic models taking into account the finite thermal conductivity, radiation transfer, and radiation absorption [2]. The only parameter determining the state of the corona $\gamma_0 = \varkappa_0^{3/4} q/(\rho_*^7 R_0^3)^{1/4} \times (M/z)^{21/8}$ depends on the power density q and the frequency of the radiation $\omega = 2\pi c/\lambda$ ($\varkappa_0 \sim 1/ze^4\Lambda n^{1/2}$ is the electronic thermal conductivity). In [4] it is shown by means of numerical modeling that under conditions of stationary irradiation and no heat conduction, taking into account the dynamics of vaporization of the matter and screening of the target by the plasma accompanying a spike of absorption in the vapor, leads to a solution in the form of a periodic regime of plasma formation, whose characteristic time is equal to the gas-dynamic time $\tau \sim R_0/c_0$ (R_0 is the size of the target and c_0 is the velocity of sound).

The second direction involves the study of nonstationary physical processes in the collisionless plasma of the corona. In one of the early works [5] on the expansion of plasma into a vacuum with isothermal electrons a self-similar solution with an exponentially decaying density and linearly growing ion velocity was constructed. In [3, 6-8] the effect of fast nonmaxwellian electrons and the multicomponent composition of ions, the motion of the ion front, and excitation of waves were studied. Experimental results on plasma flow under such conditions are presented in [9]. The expansion of a finite plasmoid was studied in [10], and the additional heating or cooling of the plasmoid was studied in [11]. All solutions obtained actually have a monotonic spatial dependence of the density of the plasma in the corona, close to the dependence in [5].

The third direction [12] involves the analysis of kinetic ionization and recombination processes, taking which into account for a laser plasma changes the relative quantities of neutrals and multiply charged ions, but does not qualitatively affect their distribution function.

The transformation of the ion distribution function $f_i(v)$ and the spatial structure of the corona accompanying a change in the duration of the laser radiation was apparently first pointed out in [1, 13]. It was shown experimentally that increasing the duration of the laser pulse in the range 0.1-1 μsec with a power density of $\sim 10^{10}$ W/cm^2 leads to a significant increase in the relative number of fast ions right up to the formation of a sharp maximum in $f_i(v)$ near the high-energy boundary of their spectrum. In space this maximum is manifested in the form of a spherical envelope of high density, containing up to 50% of the energy and up to 25% of the particles in the cloud. The thickness of the

Novosibirsk. Translated from Zhurnal Prikladnoi Mekhaniki i Tekhnicheskoi Fiziki, No. 4, pp. 3-9, July-August, 1989. Original article submitted December 9, 1987; revision submitted February 4, 1988.

0021-8944/89/3004-0509 $12.50

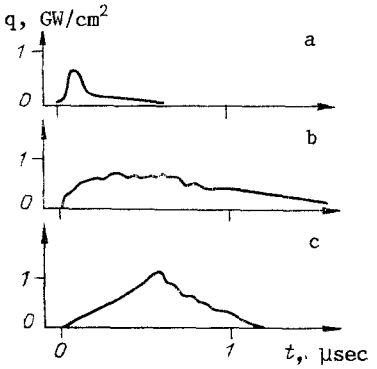

Fig. 1

envelope $\Delta R/R \leqslant 0.1$. and the envelope remains stable with expansion up to large distances. In [13] the existence of such an envelope was connected with the conditions of formation of plasma near the target.

This paper is devoted to further experimental and numerical study of the physical processes determining the observed transformation of the density distribution in a laser-produced plasma cloud and development of methods for controlling the parameters of the cloud.

Experimental Results. The experiments were performed on a KI-1 stand, which includes a vacuum chamber 1.2 m in diameter and 5 m long with a residual pressure of 10^{-4} Pa. The target consisted of a caprone filament ($C_6H_{11}ON$) with a diameter of 0.27 mm. The laser radiation (λ = 10.6 μm) was divided into two beams, which were directd onto the target from opposite radial sides. The diameter of the beams near the target was ~4 mm.

The plasma density was measured using double electric probes [14], placed at different angles and at different distances from the target. The charge and mass composition of the cloud were determined with the help of a time-of-flight analyzer [15]. The shape of the cloud was also monitored by photographing the glow of the cloud using an image-converter tube [1].

The experiments showed that when the diameter of the beam was significantly greater than the diameter of the filament, the flow was axisymmetric (the deviation was ±10%) in the plane perpendicular to the target filament. In the direction along the axis of the target, however, the ion flux decreased $j_R \sim \sin^3\theta$. The method employed to determine the total number of particles and the energy of the cloud is described in [16]. In the present experiments, like in [1, 13], the conditions of plasma formation were changed by varying the parameters of the laser radiation, typical oscillograms of which are shown in Fig. 1. The corresponding plasma density distributions $n_e(r)$ up to t = 3 μsec are presented in Fig. 2. For pulses of short duration ($\tau_r \approx 0.1$ μsec) the dependence $n_e(r)$ shows the usual decrease in the number of particles as the distance increases. However increasing τ_r while maintaining a constant power density led to a fundamental change in the structure of the laser-produced plasma (Figs. 2b and c). The cloud was characterized not only by a significant increase in the number of fast ions for velocities in the range $(0.8\text{-}1.3)\cdot 10^7$ cm/sec with q = 10^9 W/cm², but also by the formation of a sharp peak in the density on the leading edge of the cloud. It is important that light hydrogen ions and carbon ions with a maximum value for the given plasma z = 4 participated in the formation of the envelope [1]. An envelope ~2 cm thick with R ≈ 30 cm contained up to 25% of the ions and up to 50% of the energy of the cloud. Increasing τ_r up to 2-3 μsec gave a plasma flow consisting of a series of peaks (oscillogram in Fig. 3). The complicated structure of the cloud, i.e., the presence of several expanding envelopes, can be observed in its photographs [1].

All of the experimental data in aggregate suggest the following. As the pulse duration is increased the nonstationary nature of the formation of the plasma near the target, which is determined by the finite rise time of the radiation pulse τ_f, which exceeds the hydrodynamic scales $\tau_f > R_0/c_0$, and the instability of the plasma formation process [4] under the action of the radiation on the target, starts to have a significant effect on the dynamics of the plasma corona. As a result several successive axisymmetric plasmoids, expanding radially with different velocities, as well as one plasmoid with continuously varying velocity can be created. Their interaction or redistribution of the density within one of them, already occurring at the stage of inertial motion, is what leads to the restructuring of the plasma cloud.

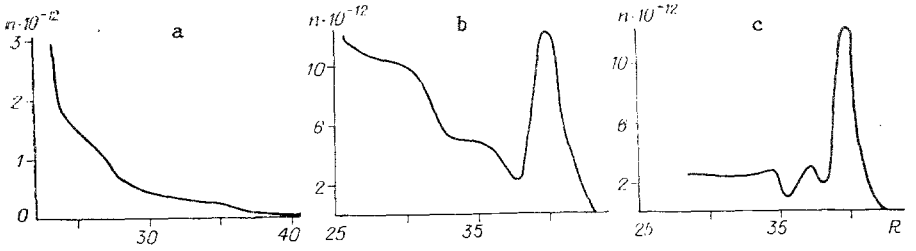

Fig. 2

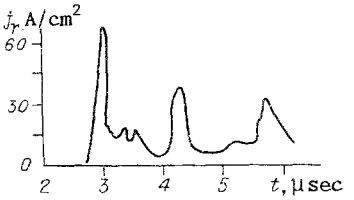

Fig. 3

Numerical Model. To study in detail the effect of nonstationary conditions of plasma production on the dynamics and structure of the corona we employed a one fluid, two-temperature hydrodynamic model. The following system of equations was solved:

$$\frac{\partial n}{\partial t}+\frac{1}{r^\nu}\frac{\partial (r^\nu nv)}{\partial r}=0,\quad \frac{\partial (nv)}{\partial t}+\frac{1}{r^\nu}\frac{\partial (r^\nu nv^2)}{\partial r}=-\frac{\partial (p_i+p_e)}{\partial r},$$
$$\frac{\partial \varepsilon_i}{\partial t}+\frac{1}{r^\nu}\frac{\partial}{\partial r}[r^\nu v(p_i+\varepsilon_i)]=-nv\frac{\partial p_e}{\partial r},\quad \varepsilon_i=\frac{nT_i}{\gamma-1}+\frac{nv^2}{2}, \tag{1}$$
$$\frac{\partial T_e}{\partial t}+v\frac{\partial T_e}{\partial r}+T_e\frac{(\gamma-1)}{r^\nu}\frac{\partial (r^\nu v)}{\partial r}=0,\quad p_e=nT_e,\quad p_i=nT_i$$

(λ = 5/3, ν = 0, 1, 2 for flat, cylindrical, and spherical symmetry, respectively). The equations are made dimensionless by scaling to the quantities R_0 – the radius of the target, T_0 – the electron temperature at the target boundary, n_*M – the critical density, and $\tau = R_0/c_0 = R_0(M/T_e)^{1/2}$ – the time scale. The problem was solved with the following boundary conditions at the target surface for a plasma source whose coordinate $r = R_0$ was assumed to be constant:

$$n|_{r=R_0}=n_*,\quad T_e=f(t),\quad v=T_e^{1/2}=f^{1/2}(t),\quad T_i=T_0. \tag{2}$$

At the boundary with the vacuum, whose position was found from the solution, it was assumed that $p_i = p_e = 0$. When the plasma source was switched off (2) was replaced by

$$\frac{\partial n}{\partial r}\Big|_{r=R_0}=\frac{\partial T_e}{\partial r}=\frac{\partial T_i}{\partial r}=0,\quad v|_{r=R_0}=0. \tag{3}$$

The system (1) with the foregoing boundary conditions is the mathematical formulation of the problem. The nostationary nature of the formation of the plasma was taken into account by changing the boundary conditions f(t).

As follows from [2], for the values of the power density of interest to us $q \lesssim 10^{11}$ W/cm², with λ = 10.6 μm, the Jouguet point R_c and the point with the critical density R_* practically coincide in space and fall near the target surface: $R_* \approx R_c \approx 1.2R_0$. For this reason the Jouguet point with the plasma velocity equal to the sound velocity and density equal to the critical density was taken as the starting point of the numerical model. For the typical starting conditions we chose $T_e = T_i$ = 30 eV and $n_* = 10^{19}$ cm^{-3}, which corresponds to $q \approx 10^{10}$ W/cm² [17]. For these parameters the path lengths $\lambda_{ee} \approx \lambda_{ei} \approx \lambda_{ii} \approx 6\cdot10^{-4}$ cm, i.e., $\lambda/R_* \ll 1$, indicating that the electronic and ionic thermal conductivities are limited and that near the target other dissipative processes are weak. For adiabatic expansion with γ = 5/3 and $T/n^{\gamma-1} \sim Tr^{4/3}$ = const we have $\lambda/r \sim T^2(nr)^{-1} \sim r^{-5/3}$. This provides a basis for

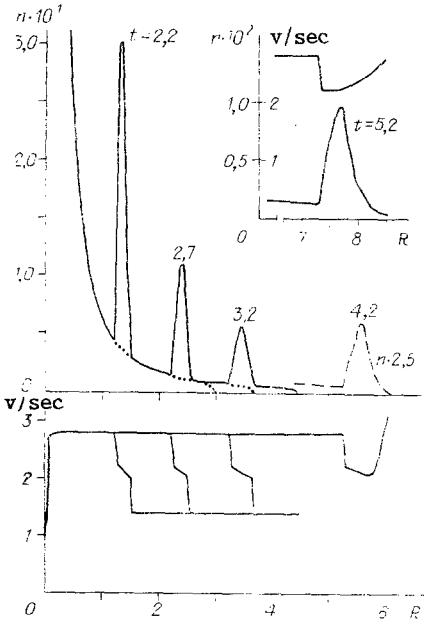

Fig. 4

regarding the plasma as collisional at large distances ($r \gg R_0$) and for using the hydrodynamic approximation (1) to describe it. The system (1) was solved numerically using a method similar to the large-particle method [18]. Its relatively high numerical viscosity must be kept in mind when analyzing the data obtained.

Results of Modeling. A. We shall first study the collision of two flows, taking the function f(t) in the form of a "step":

$$f(t) = \begin{cases} T_0, & t < \tau_0, \\ T_1, & t \geqslant \tau_0. \end{cases}$$

The solution of the problem depends on the delay time τ_0, which is uniquely related with the mass and energy of the first flow, and on the ratio of the temperatures $T = T_1/T_0$ of efflux at the Jouguet point. At the time τ_0, when the temperature changes in a jump-like fashion, a discontinuity arises; this discontinuity decays under nonstationary conditions of the expanding flows. The quantity T, which also determines at the same time the ratio of the velocities of the flows, determines the character of the decomposition. For $T < 1$ it may be expected that a region of rarefaction will appear between the outgoing flows, while for $T > 1$ a region of compression will appear.

Figure 4 shows the density and velocity distribution of the plasma in space for the spherically symmetric case with $\nu = 2$, $\tau_0 = 1.6$ and $T = 4$ in the general picture of the interaction of two flows on large space-time scales. It is obvious that the perturbation orginating at the boundary moves along the quasistationary plasma profile toward the vacuum. In the perturbation the high-velocity second flow transforms into the slow first flow. In the process of the motion the envelope arising includes the entire first flow and emerges onto the boundary with the vacuum. At this time ($t \approx 3.7$) the character of the spatial dependence of the velocity changes. The envelope formed accelerates under the action of the oncoming fast plasma and expands during the motion. The outer front of the envelope moves more rapidly than the inner front, owing to which the form of the perturbation becomes unsymmetric. The steep drop in the density on the inside and the more gentle drop on the outside qualitatively agree with the structure of the envelope observed in the experiment (see Figs. 2b and c). The velocity of the entire plasmoid asymptotically equals the velocity of the second flow, and the perturbation propagates in a stable fashion in the regime of inertial motion of the ions.

Under the conditions of outflow (2) the velocity of the moving plasma exceeds the corresponding local velocity of sound. It is well known [19] that the supersonic collision of gases leads to the formation of two shock waves (SWs), each of which moves in its own gas

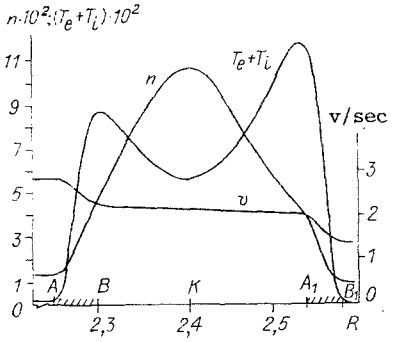

Fig. 5

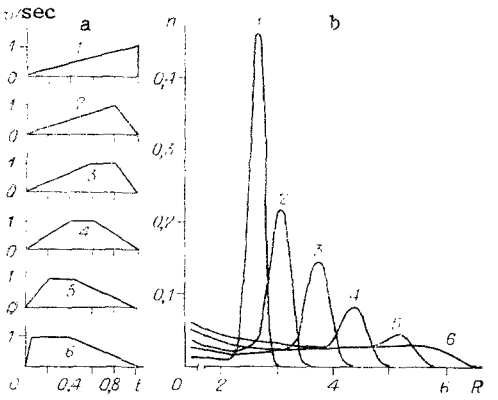

Fig. 6

away from the contact boundary. For this reason it can be expected that the transitional region between the plasma flows is confined between two SWs. The structure of the perturbation is shown in detail in Fig. 5 at the time t = 2.7. The regions AB and A_1B_1 (the fronts of the SWs smeared by the computational viscosity) and the point K (the contact boundary between the flows) can be clearly seen on the graph of the spatial distribution of the velocity. The plasma of the first N_1 and second N_2 flows, heated by the SWs, lies on both sides of the contact boundary in the perturbation. Calculations showed that before the formed envelope reaches the boundary with the vacuum the condition $N_1 \approx N_2$ holds (the deviation does not exceed 5%). This means that the mass fluxes passing through the SWs are equal. The conclusion that there are two SWs propagating away from the contact surface is confirmed by the fact that the Hugoniot conditions, calculated based on the sum of all temperatures, hold in the regions AB and A_1B_1. Thus, as an example, the value $T_2/T_1 \approx 56$ obtained in the calculations for the inner shock wave AB is equal to, within the limits of accuracy of the difference method, the temperature ratio given by the expression $T_2/T_1 = [2\gamma M_1^2 - (\gamma - 1)][(\gamma - 1)M_1^2 + 2]/(\gamma + 1)^2 M_1^2$ $(M_1 = u_1/c_1 \approx 14,$ u_1 is the velocity of the flow in front of the SW in its reference system).

For infinitely strong SWs, as $M_1 \to \infty$ and for $\gamma = 5/3$ the limiting compression of the density behind the front of the wave $\rho_2/\rho_1 = (\gamma + 1)/(\gamma - 1) = 4$. In our case after the plasma is heated by the SWs the thermal energy of the particles is transformed into the kinetic energy of directed motion of the layer of compressed plasma in the processes of adiabatic expansion of the envelope. The particles cool down, and the cooling is all the stronger the farther away they are from the shock front. The local minimum of the temperature in the perturbation is established near the contact boundary. As a result the plasma at the center of the envelope is additionally compressed to values $\rho_{max}/\rho_1 >> 4$. The cooling mechanism works most efficently (and this is confirmed by calculations) in a spherical geometry and least efficiently in a flat geometry.

B. We shall study the formation of an envelope accompanying the outflow of plasma with a finite number of particles and finite energy. Fixing the duration of the first and second flows, we change the temperature of the second flow:

$$f(t) = \begin{cases} T_0, & t < \tau_0, \\ T_1, & \tau_0 \leqslant t \leqslant \tau_1, \\ T_1(\tau_2 - t)/(\tau_2 - \tau_1), & \tau_1 \leqslant t < \tau_2, \\ (3), & t \geqslant \tau_2 \end{cases}$$

$$(\tau_0 = 0.4,\ \tau_1 = 0.8,\ \tau_2 = 1.4).$$

The computed numbers of particles N_0 and energy E_0 in the envelope as a percentage of the number of particles in the entire plasma and its energy are presented in Table 1 for different values of T_1/T_0 at the boundary at time t = 2, close to the asymptotic regime. As follows from Table 1, for $T_1/T_0 \gtrsim 2$ the parameters N_0 and E_0 are virtually independent of the ratio of the temperatures in the flows. The compression of the envelope $\Delta = \rho_{max}/\rho_1$ (the ratio of the density at the maximum to the density at the foot behind the perturbation) is also a weak function of the starting ratio of the temperatures. However the composition of

TABLE 1

T_1/T_0	N_0	E_0	N_+	E_+	Δ
	%				
1,4	50	55	44	61	1,4
2,0	52	57	52	75	2,16
3,0	53	58	58	85	2,59
4,0	53	58	62	90	2,75
5,0	53	59	66	93	2,85

TABLE 2

τ_0	N_0	E_0	N_1	E_1	Δ
	%				
0,2	48	60	39	58	2,66
0,4	64	74	52	71	4,39
0,6	73	81	59	78	6,00
0,8	79	85	65	82	7,67
1,0	82	87	68	84	9,69
1,2	84	88	70	85	12,13
1,4	86	89	71	86	14,71

the envelope changes as T_1/T_0 increases. Thus the ratio N_+ of the number of particles in the second flow contained in the envelope to the number of particles of the entire envelope grows linearly as T_1/T_0 increases (E_+ is the analogous ratio of the energies). The change in the relative fraction N_+ from 1/2 to 2/3 indicates that the second flow is efficiently stopped by the "wall" created by the first flow. For large values of the temperature ($T_1/T_0 \approx 5$) almost all of the energy of the envelope (93%) is acquired from the second flow.

We shall study the effect of the duration τ_0 of the first flow with that of the second flow held constant on the energetics of the formation of the envelope. The results are summarized in Table 2 for the close to asymptotic stage of expansion with $T_1/T_0 = 4$ and $\tau_1 = \tau_0 + 0.2$, $\tau_2 = \tau_0 + 0.8$.

The maximum compression (86% of the particles and 89% of the energy are in the envelope) was obtained with $\tau_0 = 1.4$, when the number of particles in the first flow is close to that in the second flow. This result follows in a natural fashion from the regime of formation of the envelope. As noted above, prior to emerging into the boundary with the vacuum, the envelope contains an equal amount of plasma from the first and second flows. Therefore the optimal condition for completing the process of formation of the perturbation is that the entire mass of both flows M_1 and M_2 must be expended simultaneously; this is achieved when they are equal ($M_1 \approx M_2$).

After the plasma source is switched off, the relative fraction of the second flow in the envelope depends on the result of the action of the inner rarefaction wave on it. The parameters N_1 and E_1 in Table 2 show the number of particles and the energy of the second flow, which are present in the envelope, scaled to the corresponding quantities of the entire second flow. In the calculations more than half of the pushing plasma for $\tau_0 > 0.2$ remains in the envelope, while the values $N_1 = 71\%$ and $E_1 = 86\%$ for $\tau_0 = 1.4$ show that the plasma flow is compressed in a narrow moving layer.

C. For outflow velocity varying continuously in time a group of calculations with boundary conditions in the following form was performed:

$$f(t) = \begin{cases} (T_1 - T_0)(t/\tau_0)^\alpha + T_0, & t \leqslant \tau_0, \\ T_1, & \tau_0 \leqslant t \leqslant \tau_1, \\ (T_1 - T_0)[(\tau_2 - t)/(\tau_2 - \tau_1)]^\alpha + T_0, & \tau_1 \leqslant t \leqslant \tau_2 \end{cases} \quad (T_1/T_0 = 100).$$

For $t > \tau_2$ the conditions (3) for "switching off" the plasma source are imposed. These calculations reflected most completely the character of the changes in the temperature and velocity of the plasma as the palsma is formed by a real laser pulse. The time dependence of the outflow velocity of the plasma at the boundary for $\alpha = 2$ (lines 1-6) is presented in Fig. 6a, and the corresponding spatial distributions of the plasma are presented in Fig. 6b ($t = 2$). Control variants with $\alpha = 0.25$ and 4 were qualitatively the same as the results presented. The formation of a plasma wall and stopping of the growing plasma flow on it is the main mechanism of compression of the ion flow. By changing the dynamics of the flow at the target is possible to obtain different spatial distributions of the plasma, which is achieved in the experiment by varying the shape of the laser pulse. The necessary condition for the appearance of a thin envelope is that the thermal energy liberated must be converted into the kinetic energy of expansion. In the flat case, for which the adiabatic cooling is weak, plasma compression greater than $(\gamma + 1)/(\gamma - 1)$ was not found in the calculations.

Thus we have proposed a numerical model for a new phenomenon – the compression of ions into a thin envelope in the process of expansion of a laser-produced plasma into a vacuum. We showed experimentally and theoretically that the distribution function of the ions and the spatial structure of the corona of the laser plasma can be controlled by shaping the CO_2 laser pulse in the microsecond range of pulse duration. We note that the phenomenon studied does not depend on the method employed to create the plasma flow or the energy source, but rather it is determined solely by the regime of outflow of the plasma at the boundary and by the geometry of the problem. The mathematical model studied, assuming that the temperatures of the ions and electrons are equal, describes the dynamics of the compressed gas. For this reason the conclusion regarding the mechanism of compression of matter behind the SW up to densities $\rho_2/\rho_1 = (\gamma + 1)/(\gamma - 1)$ is also correct in gas dynamics.

LITERATURE CITED

1. V. M. Antonov, Yu. P. Zakharov, et al., "Application of laser plasma for laboratory model of astrophysical process," in: Powerful CO_2 Lasers for Plasma Experiments and Technology [in Russian], Inst. Teor. Prikl. Mekh., Sib. Otd. Akad. Nauk, Novosibirsk (1986).
2. S. Yu. Gus'kov, V. V. Zverev, et al., "Acceleration and compression of spherical targets by long-wavelength laser radiation," Tr. FIAN SSSR, 170 (1986).
3. A. V. Gurevich and L. P. Pitaevskii, "Nonlinear dynamics of a rarefied plasma and ionospheric aerodynamics," in: Problems in Plasma Theory [in Russian], Atomizdat, Moscow (1980), No. 10.
4. G. G. Vilenskaya and I. V. Nemchinov, "Numerical calculations of the motion and radiation heating of a laser-produced plasma forming under conditions of a "spike" of absorption in the vapor of a solid," Zh. Prikl. Mekh. Tekh. Fiz., No. 6 (1969).
5. A. V. Gurevich, L. V. Pariiskaya, and L. P. Pitaevskii, "Self-similar motion of a rarefied plasma," Zh. Éksp. Teor. Fiz., 48, No. 2 (1965).
6. J. Denavit, "Collisionless plasma expansion of a plasma into a vacuum," Phys. Fluids, 22, No. 7 (1979).
7. N. Singh and R. W. Schunk, "Numerical calculations relevant to the initial expansion of the polar wind," J. Geophys. Res., 87, 9154 (1982).
8. U. Samir, K. H. Wright, and N. H. Stone, "The expansion of a plasma into vacuum: basic phenomena and processes and applications to space plasma physics," Rev. Geophys. Space Phys., No. 7 (1983).
9. V. G. Eselevich and V. G. Fainshtein, "Expansion of a collisionless plasma into a vacuum," Fiz. Plazmy, 7, No. 3 (1981).
10. A. V. Gurevich and A. P. Meshcherkin, "Acceleration of ions with spherical expansion of plasma," Fiz. Plazmy, 9, No. 5 (1983).
11. Yu. I. Chutov and A. Yu. Kravchenko, "Effect of additional cooling and heating of electrons on the expansion of plasmoids into a vacuum," Fiz. Plazmy, 9, No. 3 (1983).
12. Yu. A. Bykovskii, N. N. Dityarenko, et al., "Recombination in an expanding plasmoid," Zh. Tekh. Fiz., 44, No. 1 (1974).
13. A. M. Orishich, A. G. Ponomarenko, and V. N. Snytnikov, "Nonlinear transformation of ion fluxes into a thin sheath during the plasma expansion into vacuum," 7th International Conference on Plasma Physics, Kiev, 1987: Contributed Papers, Kiev (1987), Vol. 4.
14. Yu. P. Zakharov, "Characteristics of probe methods for studying the interaction of flows of laser-produced plasma with a magnetized background medium," in: Powerful CO_2 Lasers for Plasma Experiments and Technology [in Russian], Inst. Teor. Prikl. Mekh., Sib. Otd. Akad. Nauk SSSR, Novosibirsk (1986).
15. V. M. Antonov, "Characteristics of the diagnostics of the corpuscular composition and parameters of strong flows of laser plasma on the KI-1 stand," Inst. Teor. Prikl. Mekh., Sib. Otd. Akad. Nauk SSSR, Novosibirsk (1986).
16. V. M. Antonov, Yu. P. Zakharov, et al., "Creation of clouds of laser plasma with $N \sim 10^{19}$ particles," Teplofiz. Vys. Temp., 23, No. 4 (1985).
17. S. K. Goel, P. D. Gupta, and D. D. Bhawalkar, "Effect of radiation losses on scaling laws in laser-produced plasmas," J. Appl. Phys., 53, No. 1 (1982).
18. O. M. Belotserkovskii and Yu. M. Davydov, Method of Large Particles in Gas Dynamics [in Russian], Nauka, Moscow (1982).
19. L. D. Landau and E. M. Lifshitz, Hydrodynamics [in Russian], Nauka, Moscow (1986).